

RESEARCH ARTICLE

# Quercetin and aconitine synergistically induces the human cervical carcinoma HeLa cell apoptosis via endoplasmic reticulum (ER) stress pathway

Xiu-Mei Li<sup>1,2\*</sup>, Jing Liu<sup>1,2</sup>, Fang-Fang Pan<sup>3</sup>, Dong-Dong Shi<sup>1,2</sup>, Zhi-Guo Wen<sup>1,2</sup>, Pei-Long Yang<sup>1,2\*</sup>

**1** Key Laboratory for Feed Biotechnology of the Ministry of Agriculture, Feed Research Institute, Chinese Academy of Agricultural Sciences, Beijing, China, **2** National Engineering Research Center of Biological Feed, Feed Research Institute, Chinese Academy of Agricultural Sciences, Beijing, China, **3** Key Lab of Industrial Fermentation Microbiology of the Ministry of Education, Tianjin Key Lab of Industrial Microbiology, College of Biotechnology, Tianjin University of Science and Technology, Tianjin, China

\* [lixiumei@caas.cn](mailto:lixiumei@caas.cn) (XML); [yangpeilong@caas.cn](mailto:yangpeilong@caas.cn) (PLY)



**OPEN ACCESS**

**Citation:** Li X-M, Liu J, Pan F-F, Shi D-D, Wen Z-G, Yang P-L (2018) Quercetin and aconitine synergistically induces the human cervical carcinoma HeLa cell apoptosis via endoplasmic reticulum (ER) stress pathway. PLoS ONE 13(1): e0191062. <https://doi.org/10.1371/journal.pone.0191062>

**Editor:** Ying-Jan Wang, National Cheng Kung University, TAIWAN

**Received:** October 11, 2017

**Accepted:** December 26, 2017

**Published:** January 11, 2018

**Copyright:** © 2018 Li et al. This is an open access article distributed under the terms of the [Creative Commons Attribution License](https://creativecommons.org/licenses/by/4.0/), which permits unrestricted use, distribution, and reproduction in any medium, provided the original author and source are credited.

**Data Availability Statement:** All relevant data are within the paper and its Supporting Information file.

**Funding:** Our work was financially supported by the National Key Research and Development Program of China (2017YFD0400300) and the Agricultural Science and Technology Innovation Program (CAAS-XTGX2016011-04-3).

**Competing interests:** The authors have declared that no competing interests exist.

## Abstract

Up till now, studies have not been conducted on how the combination of Quercetin (Q), Aconitine (A) and apoptosis induction affects human cervical carcinoma HeLa cells. The result of our findings shows that the combination of Q and A (QA) is capable of synergistically inhibiting the proliferation of HeLa cells in a number of concentrations. QA synergistically inhibits the proliferation of MDR1 gene in the HeLa cells. It is concluded based on our result that QA induces apoptosis and ER stress just as QA-induced ER stress pathway may mediate apoptosis by upregulating mRNA expression levels of eIF2 $\alpha$ , ATF4, IRE1, XBP1, ATF6, PERK and CHOP in the HeLa cells. The up-regulating of mRNA expression level of GRP78 and activation of UPR are a molecular basis of QA-induced ER stress.

## Introduction

Cervical cancer is one of the leading causes of death among women worldwide [1]. Approximately 85% of cervical cancer cases occur in low- and middle-income countries [2]. While there are established methods of treatment for affected people, such methods possess significant side effects. Natural treatment products, on the other hand, or phytochemicals, are preferred for their safety and lower drug resistance [3]. Developing effective anti-cancer drugs from plants require great effort. Over 60% of anticancer drugs have their main ingredients from natural sources [4]. Herbal medicines fight cancer by inhibiting cell proliferation, inducing apoptosis and modulating cell signaling pathway and oxidative stress-mediated mechanism [5, 6].

Quercetin (Q), a flavonoid found in fruits, vegetables, tea and other plant-derived foods, has unique biological properties capable of improving mental/physical performance and reducing infection risk [7,8]. Q has been found to have anti-proliferative and pro-apoptotic

effects on HeLa cells [9]. It is active throughout the stages of carcinogenesis, from initiation to invasion and metastasis, and is able also to undermine the basis of the development and maintenance of tumors. PI3K/Akt pathway in HeLa cells have been found to mainly mediate the anti-proliferative and apoptotic processes caused by Q.

Aconitine (A), which is also known as monkshood or devil's helmet, is a kind of Aconitum plant-produced toxin [10]. A is often used as the antipyretic and analgesic agent in many Asian countries in spite of its cardiotoxic and neurotoxic risks. However, it is difficult to measure its appropriate dosage due to its narrow therapeutic index [11, 12].

The failure of chemotherapy-based treatment has been attributed largely to Multidrug resistance (MDR), the development of which has been linked to chemotherapeutic failure in cancer treatment. An MDR phenotype may occur from mechanisms such as alteration of drug targets, increased DNA repair, reduced cell apoptosis and overexpression of drug efflux transporters [13]. Some studies showed that overexpression of drug efflux proteins in the ATP-binding cassette superfamily, particularly P-glycoprotein (P-gp; encoded by *MDR1* or *ABCB1* gene), inhibited the intracellular accumulation of cytotoxic drugs, causing a reduction of drug-mediated cytotoxicity [14]. The cells ultimately develop resistance toward these cytotoxic drugs.

Apoptosis is a preferred method for cancer chemotherapy [15]. As suggested by recent studies, ER stress also contributes to apoptosis just as ER stress-induced apoptosis pathways have become a popular field of research [16]. The ER accurately ensures proteins are folded and assembled before they are sent to other organelles [17, 18]. ER stress occurs when abnormalities such as protein misfolding and unfolded protein accumulate in the ER lumen, resulting in the dissociation of GRP78 from the ER stress transducers and triggering the activation of the UPR branches [19–22]. ER stress-induced apoptosis can occur when UPR fails to compensate for the abnormalities [23].

In summary, the objective of this study was to evaluate the effect of Q and A in combination with apoptosis induction via endoplasmic reticulum (ER) stress pathway in human cervical carcinoma HeLa cells.

The mRNA expression of GRP78, which was the maker of ER stress was determined. The mRNA expression of UPR pathway (eIF2 $\alpha$ , ATF4, IRE1, XBP1, ATF6, PERK and CHOP) was also measured.

## Materials and methods

### Chemicals and reagents

Quercetin and Aconitine were purchased from the National Institutes for Food and Drug Control (Beijing, China).

### Cell culture

Human cervical carcinoma HeLa cells were purchased from the American Type Culture Collection (ATCC) and cultured in DMEM/F12 containing 10% FBS, 100  $\mu$ g/mL streptomycin and 100 units/mL penicillin at 37°C in a controlled condition at 5% CO<sub>2</sub> and 90% relative humidity.

### Cell viability

Cell viability effect of drug on HeLa cells was determined, with some modifications, by MTT assay as previously described [24]. HeLa cells were seeded in 96-well plates (10<sup>5</sup> cells/well) and cultured overnight. Next, the cells were treated for 48hrs using different drug concentrations. After treatment, the cells were washed twice with phosphate buffered saline (PBS) and

incubated with 20  $\mu$ L MTT (5mg/mL) and 80  $\mu$ L DMEM for 4 hrs. MTT solution was then removed and 100  $\mu$ L DMSO was added to each well. The absorbance was measured at 490 nm by Microplatereader. All the results were expressed as the inhibition ratio of cell proliferation calculated as  $[(A-B)/A] \times 100\%$ , where A and B are the average numbers of viable bacterial cells of the control and samples, respectively.

### Computation of the combination index for quantitative determination of drug interactions

In drug combination studies, many researchers are interested in quantifying drug interactions and classifying the interactions into categories of synergy, additivity, or antagonism [25]. The most widely used method for evaluating drug interactions in combination cancer chemotherapy is Combination Index (CI) analyses [25, 26]. The Loewe additivity model has been a reference model majorly used when the combined effect of two drugs is additive [25, 26]. The model can be written as in Eq (1):

$$\frac{(D)1}{(Dx)1} + \frac{(D)2}{(Dx)2} = 1 \tag{1}$$

where  $(D)_1$  and  $(D)_2$  are the respective combination doses of drug 1 and drug 2 that yield an effect of 50% growth inhibition, with  $(Dx)_1$  and  $(Dx)_2$  being the corresponding single doses of drug 1 and drug 2 that result in the same effect, which is by definition the GI50 of drug 1 and drug 2. When Eq 1 holds, it can be concluded that the combined effect of the two drugs is additive. Based on Eq 1, the combination index, defined in Eq (2), can be used to classify drug interactions as synergistic, additive, or antagonistic [25, 26].

$$CI = \frac{(D)1}{(Dx)1} + \frac{(D)2}{(Dx)2} \tag{2}$$

CI<1 synergy; CI = 1 additivity; CI>1 antagonism

A CI of less than, equal to or more than 1 indicates synergy, additivity or antagonism, respectively. We simulated isobolograms for a pair of drugs with eight equally effective dose combinations for a particular effect level of GI50. GI50 normalized doses of drug 1 and drug 2 that give this effect in combination are plotted as axial points in the isobologram graphs. According to Eq 2, the isobologram curves are expected to be parallel to the diagonal for additive drug pairs, concave for synergistic drug pairs, and convex for antagonistic drug pairs. We focused on the qualitative shape of the isobolograms to correctly identify the drug pair category, and use the smallest CI of the eight drug dose combinations as the CI for this drug pair [25, 26].

### Measurement of reactive oxygen species

According to manufactures' instructions, the level of reactive oxygen species (ROS) was measured by dichloro-dihydro-fluorescein diacetate. Briefly, cells were incubated with dichloro-dihydro-fluorescein diacetate (final concentration of 10  $\mu$ M) at 37°C in the dark for 30 minutes, then washed with cold phosphate-buffered saline (PBS), and then analyzed immediately, using a FACS.

### Cell apoptosis assay

The FITC Annexin-V/Dead Cell Apoptosis Kit with FITC annexin V and propidium iodide (PI) (Invitrogen, Molecular Probes, USA) for flow cytometry provides a rapid and convenient

assay for apoptosis. In this protocol,  $1 \times 10^5$  cells were seeded and washed twice with PBS, and then mixed with 100  $\mu$ L binding buffer to form a cell suspension. FITC annexin-V 5  $\mu$ L was mixed with 1  $\mu$ L of 100  $\mu$ g/mL PI working solution. The cells were incubated in the dark for 15 minutes at room temperature. 400  $\mu$ L binding buffer was then added, mixed gently and analyzed immediately using an FACS.

### TUNEL assay

We used in situ cell death detection kit (molecular probes, Invitrogen, USA). The method distinguishes apoptotic cells from those undergoing necrosis because damaged DNA in the former leads to a different distribution of staining and nuclear morphology. Firstly, the testis sections were fixed for one hour using 4% paraformaldehyde (PFA) and later washed three times with PBS. The sections were then submerged in PBS with 0.1% Triton-X-100 in an ice bath for 2 min. After further washes with PBS, the reaction was performed in the terminal deoxynucleotidyl transferase (TdT) buffer with fluorescein labeled dUTP. The samples were then incubated with a reagent for one hour at 37°C with plastic membrane mounted to avoid reagent evaporation. Washed with PBS, the sections were incubated with a mixture of DAPI and antifade reagent before coverglass mounting. A positive TUNEL preparation kit (Beyotime, China) was used to prepare the positive control. The sections were treated with DNase I for 30 min at 25° and PBS wash before TUNEL labeling reaction. The TUNEL results were then analyzed with a Leica scanning confocal microscope (TCS SP5) (Leica, Germany).

### Mitochondrial membrane potential ( $\Delta\psi_m$ ) assay

Flow cytometry (Bio-Rad, USA) and mitochondria-selective dye JC-1 detection kit (Molecular Probes, USA) were used to measure the mitochondrial membrane potential ( $\Delta\psi_m$ ). Mitochondrial uptake of JC-1 is dependent on its lipophilic action driven by the polarity of  $\Delta\psi_m$ . In normal mitochondria, JC-1 exists as a polymer emitting red fluorescence that can be detected by flow cytometry FL-2 channel. If  $\Delta\psi_m$  is depolarized, the JC-1 enters the mitochondria and presents as monomer green fluorescence that can be detected by FL-1 channel. The JC-1 was used to detect the mitochondrial membrane potential, an indicator of mitochondrial dysfunction and early apoptosis.

A mitochondrial membrane potential assay kit was used to detect the potential loss of mitochondrial membrane. Briefly, cells were seeded in 6-well plates at a density of  $1 \times 10^5$  cells/mL and cultured overnight, then treated with QA for 24hrs. The cells were twice washed with PBS then stained with JC-1 for 20 min at 37°C with 5% CO<sub>2</sub>-95% air. Then the cells were twice washed with JC-1 staining buffer and analyzed immediately by FCM.

### Real time polymerase chain reaction (RT-PCR)

HeLa cells were plated into six well plates at a density of  $1 \times 10^5$  cells per well. Cells were treated with QA (44.08  $\mu$ g/mL) for 24hrs after 12hrs of cultivation. Total RNA was then isolated by using Trizol reagent (Invitrogen, Carlsbad, USA). First-strand cDNA was synthesized with random hexamer primers. PCR primers specific for MDR1, IRE1 $\alpha$ , PERK, XBP1, ATF4, eIF2 $\alpha$ , GRP78, ATF6, CHOP or GAPDH, the internal control, were listed in [S1 Table](#). Briefly, the amplification of primer was carried out with 40 cycles at a melting temperature of 94° for 15secs, an annealing temperature of 60° for 1 min, and an extension temperature of 72° for 50 s. The fold or percentage of change in the relative expression of the mRNA of the target gene was measured by the  $2^{-\Delta\Delta C_t}$  method.

### Statistical analysis

All the data were expressed as mean±standard deviation. The statistical analysis was performed using one-way analysis of variance test for multiple comparisons. The differences between comparisons were considered to be statistically significant at  $P<0.05$ . SPSS software version 17.0 (SPSS Inc., Chicago, IL, USA) was used for data analysis.

## Results and discussion

### How the growth inhibition of HeLa cells is induced by the combined treatment of Q and A

First, we assessed the effect of Q or A as a single agent in the growth of the HeLa cells. Either Q or A is able to individually cause a markedly dose-dependent reduction in cell viability, with 50% growth inhibition ( $IC_{50}$ ) of 55.99  $\mu\text{g/mL}$  (Fig 1A) and 71.89  $\mu\text{g/mL}$  (Fig 1B), respectively. Next, we attempt to estimate the combined effect of Q and A on HeLa cell viability by adopting a combination treatment, using varying concentrations of Q (0–100  $\mu\text{g/mL}$ ), together with varying concentrations of A (0–100  $\mu\text{g/mL}$ ) at 1:1 concentration ratio. In the end, the combined treatment of Q and A substantially inhibited HeLa cell growth as against single drug alone. Fig 1C showed 0.78-fold and 0.61-fold decrease of  $IC_{50}$  compared to Q or A treatment alone, indicating that the combination treatment with Q and A is more effective in inhibiting the growth of HeLa cells than either Q or A alone.

To evaluate their synergistic effect on HeLa cells, we assessed synergy using CalcuSyn software to evaluate the combination index originally described by Chou and Talalay, where synergism, additivity and antagonism are defined as  $CI<1$ ,  $CI = 1$  and  $CI>1$ , respectively [25].

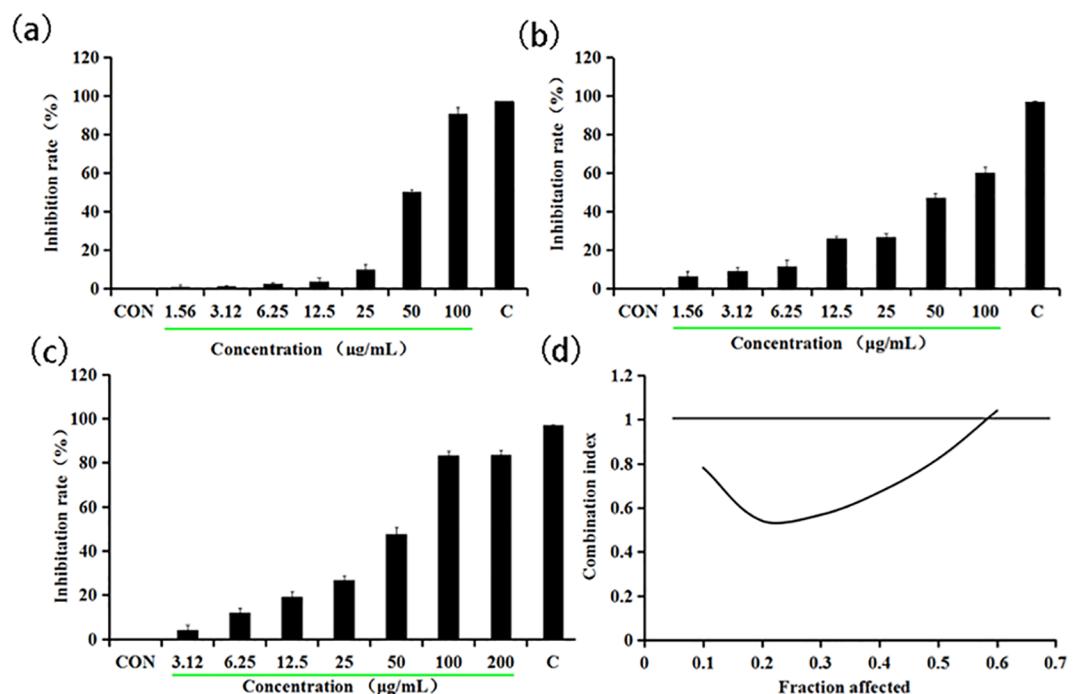


**Fig 1. Quercetin combined with aconitine inhibit HeLa cell proliferation.** (a) Quercetin inhibits HeLa cell proliferation. (b) Aconitine inhibits HeLa cells proliferation. (c) Quercetin combined with aconitine inhibit HeLa cells proliferation. (d) Median effect analysis of curcumin in combination with Q and A.

<https://doi.org/10.1371/journal.pone.0191062.g001>

The CI value was nearly 0.6 when HeLa cells were exposed to the combination of 61.75  $\mu\text{g}/\text{mL}$  QA, indicating a slight antagonism (Fig 1D). However, HeLa cells, upon exposure to the combination of variable concentrations of QA (0–61.75  $\mu\text{g}/\text{mL}$ ), demonstrated clear evidence of synergy since the CI value ranged from 0.1 to 0.6 (Fig 1D).

Q, found in the plants, such as vegetables and fruits, is becoming a major field of research because of its potential health benefits and minimal side effects [9]. It has been reported to have the antiproliferative and proapoptotic effects on HeLa cells. It is also an anti-tumor agent, which works on virtually all the stages of carcinogenesis and can undermine the basis of the development and maintenance of tumors [9]. A, also known as monkshood or devil's helmet, is an Aconitum plant-produced toxin. It is commonly used as a traditional medicine in China because of its analgesic and anti-inflammatory activities, in spite of its narrow therapeutic index.

### QA synergistically inhibits the proliferation by MDR1 gene in the HeLa cells

The failure of chemotherapy-based treatment occurs majorly because of MDR. Of the many mechanisms of MDR, the high expression of the human MDR1 gene and the P-glycoprotein (P-gp) transporter encoded by MDR1 attract the highest level of scrutiny among researchers [27]. Tumor cells that overexpress MDR1/P-gp usually show resistance to various chemotherapeutics. From Fig 2, we see that all of the results showed that the expression of MDR1 mRNA level decreased in the Q (0.79 $\pm$ 0.03), A (0.85 $\pm$ 0.04) and QA (0.54 $\pm$ 0.02) groups, whereas the QA (0.54 $\pm$ 0.02) group showed a better effect. Furthermore, previous study have shown that Q inhibits the expression of P-gp. It is able to reduce the degradation rate of the drug in the body and the cells, so as to improve the intake rate of tumor tissue on drug [28].

### QA induces HeLa cell apoptosis

**Reactive oxygen species.** ROS generation is one of the events that take place at the onset of apoptosis [29]. As shown in Fig 3, incubating HeLa cells with QA (44.08 $\mu\text{g}/\text{mL}$ ) for 24 hrs at 37°C caused a significant increase in DCF fluorescence. It is suggested that ROS is generated by many anticancer drugs by causing oxidative stress and inducing apoptosis in cancer cells, while many inhibitors of apoptosis have antioxidant activity [30]. Indeed, factors that cause or

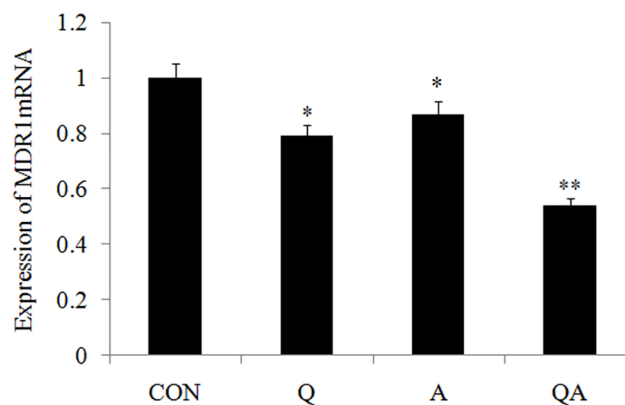


**Fig 2.** (a-c) RT-PCR was performed to examine the effect of Q, A and QA on the mRNA expression of MDR1. GAPDH served as an internal control. Data are presented with mean $\pm$ standard deviation (n = 5) \* $p$ <0.05, compared with the control group; \*\* $p$ <0.01, compared with the control group.

<https://doi.org/10.1371/journal.pone.0191062.g002>

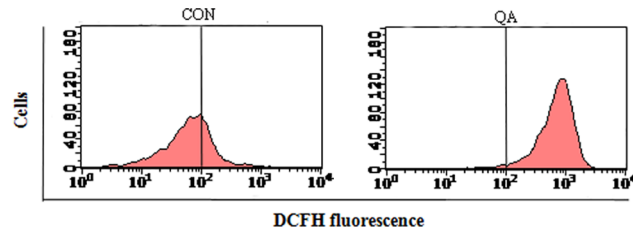


**Fig 3. Effect of QA on the intracellular ROS generation in HeLa cells.** Cells were stained using DCHF2-DA and then analyzed using a flow cytometer.

<https://doi.org/10.1371/journal.pone.0191062.g003>

promote oxidative stress, such as ROS production, lipid peroxidation and the down-regulation of antioxidant genes, are involved in apoptotic processes [31]. By inducing mitochondrial membrane damage, ROS induction up-regulates the activity of certain enzymes that are involved in the cell-death pathway [29]. With these results, we established that QA treatment induced the growth inhibition and ROS generation in HeLa cells, indicating that ROS production was the likely cause of QA-induced apoptosis.

**Cell apoptosis assay.** Annexin-V/PI double staining was used to differentiate intact cells from early apoptotic cells, late apoptotic cells, and dead (necrotic) cells as well as to investigate apoptosis in greater detail [32]. Fig 4 quantifies the increase in apoptotic cell labeling with Annexin V<sup>+</sup>/PI<sup>-</sup>, which increases from 11.38% in the control group to 80.04% in the QA-treated group. Taken together, these observations suggested that QA significantly stimulated apoptosis in HeLa cells.

**TUNEL assay.** The TUNEL assay can detect DNA strand breaks that are mainly induced by reactive oxygen species (ROS) and abortive apoptosis. To confirm that QA is connected to late apoptosis in HeLa cells, DNA damage and nuclear fragmentation in HeLa cells were analyzed by TUNEL and DAPI staining, respectively (Fig 5). Through confocal microscopy observation, the cells with QA showed a strong green fluorescence or green fluorescent spots, which indicated DNA fragmentation (Fig 5). These findings were further corroborated with those of DAPI staining, as DAPI binds to AT sites on the minor groove of DNA and emits fluorescence. Similarly, it was found that HeLa cells exposed to QA had a DAPI-positive phenotype and showed chromatin condensation, indicating nuclear fragmentation. We established from our results that QA induced changes in the structure and content of the nuclear DNA of HeLa cells (Fig 5).

**Mitochondrial membrane potential.** Mitochondrial membrane is usually damaged by excess ROS generation and this can lead to cell death [33, 34]. Mitochondrial dysfunction,

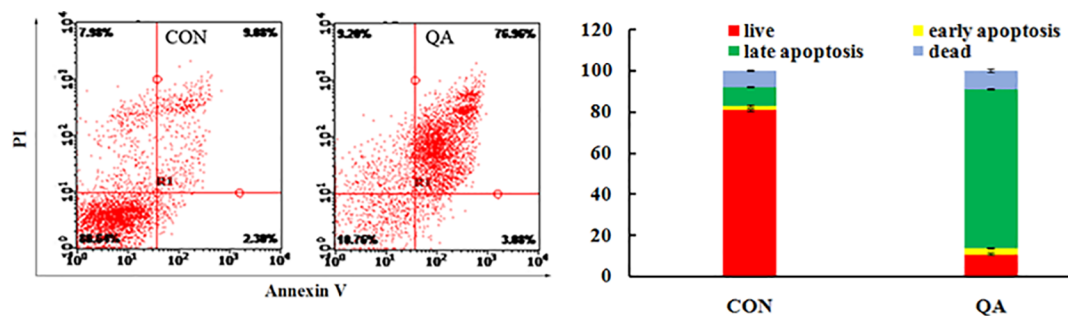


**Fig 4. Analysis of cell apoptosis.** (a) Flow cytometric measure of PS externalization in HeLa cells. (b) Representation of the frequency of live, early apoptotic, late apoptotic and necrotic cells from (a).

<https://doi.org/10.1371/journal.pone.0191062.g004>

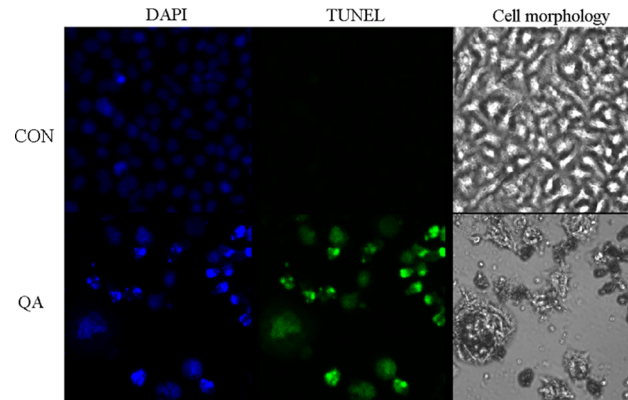


**Fig 5. DNA and nuclear damage by QA was measured by fluorescence microscopy using TUNEL and DAPI staining in cells.**

<https://doi.org/10.1371/journal.pone.0191062.g005>

including the loss of mitochondrial membrane potential ( $\Delta\Psi_m$ ) and the release of cytochrome c from the mitochondria into the cytosol, is associated with apoptosis [35]. We, therefore, examined whether QA-induced ROS generation could trigger mitochondrial membrane damage in HeLa cells. After being treated with QA (44.08  $\mu\text{g}/\text{mL}$ ) for 24 hours, HeLa cells were stained with a membrane potential indicator JC-1. The mitochondrial membrane potential was then analyzed by FCM. QA treatment resulted in a significant loss of mitochondrial membrane potential, as shown in Fig 6, indicating that QA can induce mitochondrial dysfunction from  $3.08 \pm 0.62\%$  to  $23.04 \pm 1.14\%$  in HeLa cells. These data suggested that the augment of intracellular ROS generation induced by QA might be an upstream event of mitochondrial membrane potential.

**QA induces ER stress by activating UPR pathways in the HeLa cells.** It has been demonstrated by some studies that an ER chaperone protein GRP78 serves as a master UPR regulator and plays essential roles in activating PERK, IRE1, and ATF6, in response to ER stress [36]. GRP78, also known as BiP, is a multi-functional protein predominantly expressed in the lumen of the ER. Typically, GRP78 acts as a major ER chaperone and a master regulator of ER stress signaling through controlling protein folding and assembly, preventing protein aggregation, and regulating signaling of the unfolded protein response [37–43]. First, we examined whether QA could induce ER stress in the HeLa cells. We examined the mRNA expression of GRP78, which was the marker of ER stress. As shown in Fig 7A, GRP78 mRNA expression

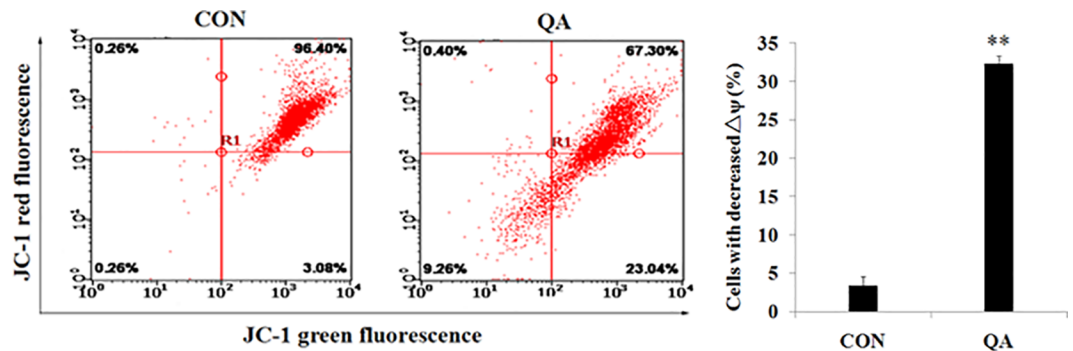


**Fig 6. (a,b) Effect of QA on the  $\Delta\Psi_m$  in HeLa cells. Cells were stained using JC-1 and then analyzed using a flow cytometer.**

<https://doi.org/10.1371/journal.pone.0191062.g006>



was significantly higher ( $p < 0.05$  or  $p < 0.01$ ) in the QA-treated group ( $1.58 \pm 0.09$ ) than it was in the control group ( $1.00 \pm 0.04$ ). We examined all the three UPR pathways—PERK pathway, IRE1 pathway and ATF6 pathway—to further confirm that UPR pathways were involved in QA-induced ER stress. In Fig 7B–7H, eIF2 $\alpha$  ( $1.95 \pm 0.08$ ), ATF4 ( $2.16 \pm 0.10$ ), IRE1 ( $1.81 \pm 0.07$ ), XBP1 ( $3.23 \pm 0.02$ ), ATF6 ( $1.82 \pm 0.01$ ), PERK ( $1.31 \pm 0.09$ ) and CHOP ( $1.11 \pm 0.05$ ) mRNA expression was significantly higher ( $p < 0.05$  or  $p < 0.01$ ) in the QA groups than that in the control group ( $1.00 \pm 0.04$ ).

UPR is a defense mechanism against various cellular stress causing accumulation of unfolded proteins in the ER [44]. The chaperone protein GRP78 is a major regulator of all three UPR pathways—PERK pathway, IRE1 pathway and ATF6 pathway—which we also monitored. Under physiological conditions, the luminal domains of PERK, IRE1 and ATF6 proteins are kept inactive when bound to the ER resident chaperone GRP78 [45]. With the accumulation of unfolded proteins, GRP78 releases enable PERK dimerization and activation to phosphorylate eIF2 $\alpha$ . The phosphorylated eIF2 $\alpha$  then induces the translation of ATF4 mRNA [46]. In this study, the results showed that QA increased the eIF2 $\alpha$  and ATF4 mRNA expression, which means that PERK pathway, is one of the mechanisms of QA-induced ER stress. ATF4 promotes many adaptive responses that restore ER function and maintain cell survival [47]. It also promotes apoptosis by regulating the CHOP and Noxa [48]. It is found that QA also activated IRE1 pathway, which was characterized by increasing the IRE1 and XBP1 mRNA expression. GRP78 is released from IRE1 and permitted to dimerize activating XBP1 kinase and

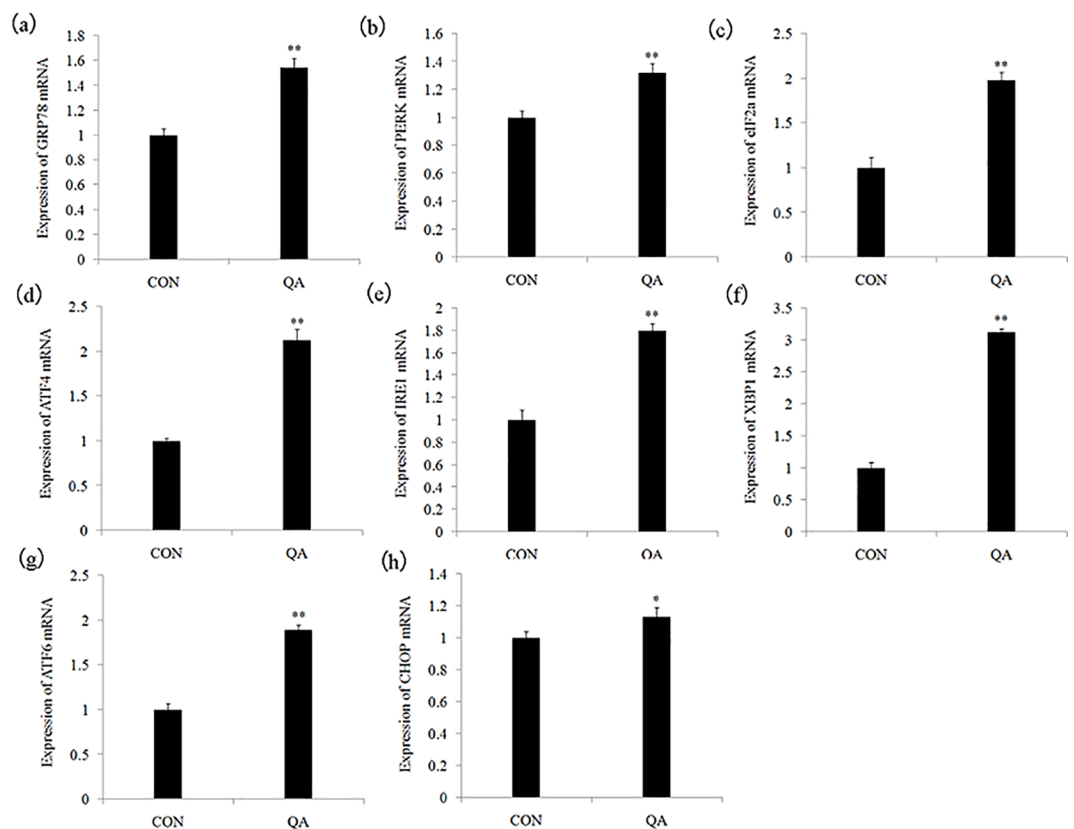


**Fig 7.** (a-h) RT-PCR was performed to examine the effect of QA on the mRNA expression of GRP78, IRE1 $\alpha$ , PERK, XBP1, ATF4, eIF2 $\alpha$ , ATF6, CHOP in HeLa cells. GAPDH served as an internal control. Data are presented with mean  $\pm$  standard deviation (n = 5) \* $p < 0.05$ , compared with the control group; \*\* $p < 0.01$ , compared with the control group.

<https://doi.org/10.1371/journal.pone.0191062.g007>

RNase activities to initiate XBP1 mRNA splice. This produces a potent transcriptional activator [49]. The XBP1 mRNA expression levels are increased in QA-treated HeLa cells. Concurrently, the increase of ATF6 mRNA expression showed that QA activated the ATF6 pathway [50].

## Conclusions

Based on our findings, we conclude that Q combined with A synergistically inhibits the proliferation of HeLa cells in a wide range of concentrations. QA synergistically inhibits the proliferation by the MDR1 gene in the HeLa cells. Our results suggest that QA induces apoptosis and ER stress just as QA-induced ER stress pathway may mediate apoptosis by upregulating mRNA expression levels of eIF2 $\alpha$ , ATF4, IRE1, XBP1, ATF6, PERK and CHOP in the HeLa cells. The upregulating of the mRNA expression level of GRP78 and the activation of UPR are a molecular basis of QA-induced ER stress.

## Supporting information

**S1 Table. Primers used for RT-PCR.** (DOC)  
(DOC)

## Author Contributions

**Conceptualization:** Xiu-Mei Li, Pei-Long Yang.

**Data curation:** Xiu-Mei Li.

**Investigation:** Xiu-Mei Li, Jing Liu, Fang-Fang Pan.

**Software:** Zhi-Guo Wen.

**Validation:** Dong-Dong Shi.

**Writing – original draft:** Xiu-Mei Li.

**Writing – review & editing:** Xiu-Mei Li, Pei-Long Yang.

## References

1. Shang HS, Chang CH, Chou YR, Yeh MY, Au MK, Lu HF, et al. Curcumin causes DNA damage and affects associated protein expression in HeLa human cervical cancer cells. *Oncol Rep.* 2016; 2016: 2207–2215.
2. Gally C, Girardet A, Viviano M, Catarino R, Benski AC, Tran PL, et al. Cervical cancer screening in low-resource settings: A smartphone image application as an alternative to colposcopy. *Clinical Trial Report.* 2017; 2017: 455–461.
3. Efferth T, Kahl S, Paulus K, Adams M, Rauh R, Boechzelt H, et al. Phytochemistry and pharmacogenomics of natural products derived from traditional Chinese medicine and Chinese materia medica with activity against tumor cells. *Mol Cancer Therapeutics.* 2008; 7: 152–161.
4. Cragg GM, Newman DJ. Plants as a source of anti-cancer agents. *J Ethnopharmacol.* 2005; 100: 72–79.
5. Hanahan D, Weinberg RA. The Hallmarks of Cancer. *Cell.* 2000; 100: 57–70. PMID: [10647931](https://pubmed.ncbi.nlm.nih.gov/10647931/)
6. Li-Weber M. Targeting apoptosis pathways in cancer by Chinese medicine. *Cancer Lett.* 2013; 332: 304–312. <https://doi.org/10.1016/j.canlet.2010.07.015> PMID: [20685036](https://pubmed.ncbi.nlm.nih.gov/20685036/)
7. Liu Y, Yang ZY, Gong C, Zhang LY, Yu GL, Gong W. Quercetin enhances apoptotic effect of tumor necrosis factor-related apoptosis-inducing ligand (TRAIL) in ovarian cancer cells through reactive oxygen species (ROS) mediated CCAAT enhancer binding protein homologous protein (CHOP)-death receptor 5 pathway. *Cancer Sci.* 2014; 105: 520–527. <https://doi.org/10.1111/cas.12395> PMID: [24612139](https://pubmed.ncbi.nlm.nih.gov/24612139/)

8. Guo WK, Ding JX, Zhang AH, Dai WD, Liu S, Diao ZL, et al. The inhibitory effect of quercetin on asymmetric dimethylarginine-induced apoptosis is mediated by the endoplasmic reticulum stress pathway in glomerular endothelial cells. *Int J Mol Sci*. 2014; 15: 484–503. <https://doi.org/10.3390/ijms15010484> PMID: 24451129
9. Xiang T, Fang Y, Wang SX. Quercetin Suppresses HeLa Cells by Blocking PI3K/Akt Pathway. *Journal of Huazhong University Science Technology*, 2014; 34: 740–744.
10. Ke LJ, Gao GZ, Shen Y, Zhou JW, Rao PF. Encapsulation of aconitine in self-assembled licorice protein nanoparticles reduces the toxicity in vivo. *Nanoscale Res Lett*. 2015; 10: 449–457. <https://doi.org/10.1186/s11671-015-1155-1> PMID: 26586149
11. Chan TYK. aconitum alkaloid content and the high toxicity of aconite tincture. *Forensic Sci Int*. 2012; 222: 1–3. <https://doi.org/10.1016/j.forsciint.2012.02.026> PMID: 22469654
12. Chan TYK. Aconite poisoning. *Clin Toxicol*. 2009; 47: 279–285.
13. Wang NB, Zhang QX, Ning BL, Luo LY, Fang YQ.  $\beta$ -Asarone promotes Temozolomide's entry into glioma cells and decreases the expression of P-glycoprotein and MDR1. *Biomed Pharmacother*. 2017; 90: 368–374. <https://doi.org/10.1016/j.biopha.2017.03.083> PMID: 28380412
14. Coley HM. Overcoming multidrug resistance in cancer: Clinical studies of p-glycoprotein inhibitors. *Methods Mol Biol*. 2010; 596: 341–358. [https://doi.org/10.1007/978-1-60761-416-6\\_15](https://doi.org/10.1007/978-1-60761-416-6_15) PMID: 19949931
15. Hengartner MO. The biochemistry of apoptosis. *Nature*. 2000; 407: 770–776. <https://doi.org/10.1038/35037710> PMID: 11048727
16. Liu H, Zeng Q, Cui Y, Zhao L, Zhang L, Fu G, et al. The role of the IRE1 pathway in excessive iodide- and/or fluoride-induced apoptosis in Nthy-ori 3–1 cells in vitro. *Toxicol Lett*. 2014; 224: 341–348. <https://doi.org/10.1016/j.toxlet.2013.11.001> PMID: 24231001
17. Zhang SX, Sanders E, Fliesler SJ, Wang JJ. Endoplasmic reticulum stress and the unfolded protein responses in retinal degeneration. *Exp Eye Res*. 2014; 125: 30–40. <https://doi.org/10.1016/j.exer.2014.04.015> PMID: 24792589
18. Deng HD, Kuang P, Cui HG, Chen L, Luo Q, Fang J, et al. Sodium fluoride (NaF) induces the splenic apoptosis via endoplasmic reticulum (ER) stress pathway in vivo and in vitro. *Aging*. 2016; 8: 3553–3567.
19. Faitova J, Krekac D, Hrstka R, Vojtesek B. Endoplasmic reticulum stress and apoptosis. *Cell Mol Biol Lett*. 2006; 11: 488–505. <https://doi.org/10.2478/s11658-006-0040-4> PMID: 16977377
20. Schröder M, Kaufman RJ. ER stress and the unfolded protein response. *Mutat Res*. 2005; 569: 29–63. <https://doi.org/10.1016/j.mrfmmm.2004.06.056> PMID: 15603751
21. Schröder M, Kaufman RJ. The mammalian unfolded protein response. *Annu Rev Biochem*. 2005; 74: 739–789. <https://doi.org/10.1146/annurev.biochem.73.011303.074134> PMID: 15952902
22. Haze K, Okada T, Yoshida H, Yanagi H, Yura T, Negishi M, et al. Identification of the G13 (cAMP-response-element-binding protein-related protein) gene product related to activating transcription factor 6 as a transcriptional activator of the mammalian unfolded protein response. *Biochem J*. 2001; 355: 19–28. PMID: 11256944
23. Jiang C, Zhang S, Liu H, Zeng Q, Xia T, Chen Y, et al. The role of the IRE1 pathway in PBDE-47-induced toxicity in human neuroblastoma SH-SY5Y cells in vitro. *Toxicol Lett*. 2012; 211: 325–333. <https://doi.org/10.1016/j.toxlet.2012.04.009> PMID: 22543052
24. Sreejith PS, Asha VV. Glycopentalone, a novel compound from *Glycosmis pentaphylla* (Retz.) Correa with potent anti-hepatocellular carcinoma activity. *J Ethnopharmacol*. 2015; 172: 38–43. <https://doi.org/10.1016/j.jep.2015.05.051> PMID: 26068427
25. Chou TC, Talalay P. Quantitative analysis of dose-effect relationships: The combined effects of multiple drugs or enzyme inhibitors. *Adv Enzyme Regul*. 1984; 22: 27–55. PMID: 6382953
26. Meng G, Wang W, Chai KQ, Yang SW, Li FQ, Jiang K. Combination treatment with triptolide and hydroxycamptothecin synergistically enhances apoptosis in A549 lung adenocarcinoma cells through PP2A-regulated ERK, p38 MAPKs and Akt signaling pathways. *Int J Oncol*. 2015; 46: 1007–1017. <https://doi.org/10.3892/ijo.2015.2814> PMID: 25573072
27. Chen J, Ding Z, Peng Y, Pan F, Li J, Zou L, et al. HIF-1 $\alpha$  inhibition reverses multidrug resistance in colon cancer cells via downregulation of MDR1/P-glycoprotein. *PLoS One*. 2014; 9: e98882. <https://doi.org/10.1371/journal.pone.0098882> PMID: 24901645
28. Yang Y, Zhang W, Huang LQ, Tao L. Effect of Quercetin Combined with Cisplatin on the Proliferation and Apoptosis of Cervical Cancer HeLa Cells. *Med J Wuhan University*. 2009; 30: 334–336.
29. Smith HO, Tiffany MF, Qualls CR, Key CR. The rising incidence of adenocarcinoma relative to squamous cell carcinoma of the uterine cervix in the United States—a 24-year population-based study. *Gynecol Oncol*. 2000; 78: 97–105. <https://doi.org/10.1006/gyno.2000.5826> PMID: 10926787

30. Ozben T. Oxidative stress and apoptosis: Impact on cancer therapy. *Pharmacists Association J Pharm Sci.* 2007; 96: 2181–2196.
31. Barrera G. Oxidative Stress and Lipid Peroxidation Products in Cancer Progression and Therapy. *ISRN Oncology.* 2012; 2012: 1–21.
32. Rieger AM, Nelson KL, Konowalchuk JD, Barreda DR. Modified annexin V/propidium iodide apoptosis assay for accurate assessment of cell death. *J Vis Exp.* 2011; 50: 2597.
33. Hseu YC, Lee CC, Chen YC, Senthil Kumar KJ, Chen CS, Huang YC, et al. The anti-tumor activity of *Antrodia salmonea* in human promyelocytic leukemia (HL-60) cells is mediated via the induction of G1 cell-cycle arrest and apoptosis in vitro or in vivo. *J Ethnopharmacol.* 2014; 153: 499–510. <https://doi.org/10.1016/j.jep.2014.03.012> PMID: 24631961
34. Kroemer G, Galluzzi L, Brenner C. Mitochondrial membrane permeabilization in cell death. *Physiol Rev.* 2007; 87: 99–163. <https://doi.org/10.1152/physrev.00013.2006> PMID: 17237344
35. Fulda S, Debatin KM. Extrinsic versus intrinsic apoptosis pathways in anticancer chemotherapy. *Oncogene.* 2006; 25: 4798–4811. <https://doi.org/10.1038/sj.onc.1209608> PMID: 16892092
36. Bernales S, Papa FR, Walter P. Intracellular signaling by the unfolded protein response. *Annu Rev Cell Dev Biol.* 2006; 22: 487–508. <https://doi.org/10.1146/annurev.cellbio.21.122303.120200> PMID: 16822172
37. Dudek J, Benedix J, Cappel S, Greiner M, Jalal C, Müller L, et al. Functions and pathologies of BiP and its interaction partners. *Cell Mol Life Sci.* 2009; 66: 1556–1569. <https://doi.org/10.1007/s00018-009-8745-y> PMID: 19151922
38. Susuki S, Sato T, Miyata M, Momohara M, Suico MA, Shuto T, et al. The endoplasmic reticulum-associated degradation of transthyretin variants is negatively regulated by BiP in mammalian cells. *J Biol Chem.* 2009; 284: 8312–8321. <https://doi.org/10.1074/jbc.M809354200> PMID: 19188365
39. Wisniewska M, Karlberg T, Lehtio L, Johansson I, Kotenyova T, Moche M, et al. Crystal structures of the ATPase domains of four human Hsp70 isoforms: HSPA1L/Hsp70-hom, HSPA2/Hsp70-2, HSPA6/Hsp70B', and HSPA5/BiP/GRP78. *PLoS One.* 2010; 5: e8625. <https://doi.org/10.1371/journal.pone.0008625> PMID: 20072699
40. Sano R, Reed JC. ER stress-induced cell death mechanisms. *Biochim Biophys Acta.* 2013; 1833: 3460–3470. <https://doi.org/10.1016/j.bbamcr.2013.06.028> PMID: 23850759
41. Xiong ZY, Jiang R, Li XZ, Liu YN, Guo FJ. Different roles of GRP78 on cell proliferation and apoptosis in cartilage development. *Int. J. Mol. Sci.* 2015; 16: 21153–21176. <https://doi.org/10.3390/ijms160921153> PMID: 26370957
42. Hardy B, Raiter A. Peptide-binding heat shock protein GRP78 protects cardiomyocytes from hypoxia-induced apoptosis. *J Mol Med.* 2010; 88: 1157–1167. <https://doi.org/10.1007/s00109-010-0657-7> PMID: 20664993
43. Liu L, Zhang Y, Gu H, Zhang K, Ma L. Fluorosis induces endoplasmic reticulum stress and apoptosis in osteoblasts in vivo. *Biol. Trace. Elem. Res.* 2015; 164: 64–71. <https://doi.org/10.1007/s12011-014-0192-4> PMID: 25434583
44. Guo HR, Cui HG, Peng X, Fang J, Zuo ZC, Deng JL, et al. Nickel chloride (NiCl<sub>2</sub>) induces endoplasmic reticulum (ER) stress by activating UPR pathways in the kidney of broiler chickens. *Oncotarget.* 2016; 7: 17508–17519. <https://doi.org/10.18632/oncotarget.7919> PMID: 26956054
45. Hetz C. The unfolded protein response: Controlling cell fate decisions under ER stress and beyond. *Nat Rev Mol Cell Biol.* 2012; 13: 89–102. <https://doi.org/10.1038/nrm3270> PMID: 22251901
46. Walter P, Ron D. The unfolded protein response: From stress pathway to homeostatic regulation. *Sci.* 2011; 334: 1081–1086.
47. Ohoka N, Yoshii S, Hattori T, Onozaki K, Hayashi H. TRB3, a novel ER stress-inducible gene, is induced via ATF4-CHOP pathway and is involved in cell death. *EMBO J.* 2005; 24: 1243–1255. <https://doi.org/10.1038/sj.emboj.7600596> PMID: 15775988
48. Gautam S, Kirschnek S, Wiesmeier M, Vier J, Hacker G. Roscovitine-induced apoptosis in neutrophils and neutrophil progenitors is regulated by the Bcl-2-family members Bim, Puma, Noxa and Mcl-1. *Plos One.* 2013; 8: e79352. <https://doi.org/10.1371/journal.pone.0079352> PMID: 24223929
49. Yoshida H, Matsui T, Yamamoto A, Okada T, Mori K. XBP1 mRNA is induced by ATF6 and spliced by IRE1 in response to ER stress to produce a highly active transcription factor. *Cell.* 2001; 107: 881–891. PMID: 11779464
50. Ron D, Walter P. Signal integration in the endoplasmic reticulum unfolded protein response. *Nat Rev Mol Cell Biol.* 2007; 8: 519–529. <https://doi.org/10.1038/nrm2199> PMID: 17565364